Vanadium-Incorporated MCM-48 Materials: Optimization of the Synthesis Procedure and an in Situ Spectroscopic Study of the Vanadium Species

M. Mathieu,*,† P. Van Der Voort,† B. M. Weckhuysen,‡ R. R. Rao,‡ G. Catana,‡ R. A. Schoonheydt,‡ and E. F. Vansant†

Laboratory of Adsorption and Catalysis, Department of Chemistry, University of Antwerpen (U.I.A.), Universiteitsplein 1, B-2610 Wilrijk, Belgium, and Centrum voor Oppervlaktechemie en Katalyse, Departement Interfasechemie, K. U. Leuven, Kardinaal Mercierlaan 92, B-3001 Heverlee, Belgium

Received: August 30, 2000; In Final Form: December 17, 2000

Highly crystalline and porous vanadium-incorporated MCM-48 materials were prepared using gemini surfactants as structure-directing agents and vanadyl sulfate pentahydrate as the source of the heteroelements. Materials with Si/V ratios varying from 20 to 100 were synthesized without loss of the typical cubic MCM-48 structure. The synthesis conditions were optimized to yield reproducible V−MCM-48 materials of high quality. The resulting materials are thoroughly characterized by UV−vis diffuse reflectance, electron spin resonance, Raman, and Fourier transform infrared spectroscopies. It was proven that the V ions in the MCM-48 are present as isolated surface species and as incorporated species in the silica matrix. For the first time, both chemical and spectroscopic tools were employed to distinguish the incorporated V sites (which are present inside the silica walls) and species that are situated externally on the surface. A fairly low amount (1 wt %) of V species is really incorporated, but these species are extremely stable, and do not leach, whereas the surface species are easily lost in aqueous media.

Introduction

The discovery of the mesoporous M41S materials has expanded significantly the possibilities for processing bulky molecules for catalytic and adsorption purposes.[1−3] In the early years, the main emphasis was on the optimization of the synthesis of the M41S materials. Especially the reproducible synthesis of MCM-48 has been an important difficulty. In the past few years, our research group[4] has found elegant ways to synthesize high-quality MCM-48. Moreover, numerous reports have appeared lately on the successful modification with catalytically active transition metals or transition metal oxides of the mesoporous, pure silica M41S materials, although most activation methods focus on the postsynthesis impregnation or the surface grafting of the active compound.[5−10] However, it has been argued that incorporated heteroelements are more stable than surface species and would not leach so easily, which is an important advantage in liquid-phase catalysis.[10]

Moreover, in the specific case of V catalysts, the activity and selectivity of these V-containing oxidation catalysts are very sensitive to the nature and coordination of the V ions.[11,12]

Only a few reports have appeared on the direct incorporation of V in M41S materials. Reddy et al.[13] studied vanadium-incorporated MCM-41 materials by ^{51}V NMR and concluded that vanadium was atomically dispersed in tetrahedral positions with a unit cell parameter a_0 of 37 Å. A more complete characterization of the coordination of vanadium-containing mesoporous molecular MCM-41 sieves was accomplished by Gontier and Tuel.[14] They noticed that the vanadium content and the template chain length of the used surfactant influence the nature and coordination of vanadium ions in these materials. The V centers of calcined and as-synthesized V−MCM-41 had the same coordination state, and no direct chemical bonding to the silicate framework was observed. A distinction between the locations of the V ions in V−MCM-41 was achieved in the work of Luan et al.[15] The 275 and 340 nm O → V charge-transfer bands were applied to determine whether the V sites are located inside or on the walls of the MCM structure. However, the assignment of the above-mentioned transfer bands has been a source of discussion in the literature. According to some authors,[16−18] the bands should be assigned to monomeric and oligomeric tetrahedral V^{5+} species, respectively. According to others[5,15,19] both bands should be assigned to monomeric tetrahedral V^{5+} species, and some authors even assign the 340 nm band to 5-fold coordinated V species.[20]

Until now, only Zhang et al.[10] reported on the incorporation of V into MCM-48 materials, using cetyltrimethylammonium bromide and vanadyl sulfate pentahydrate as vanadium source with a synthesis time of 10 days. Using ^{51}V NMR spectroscopy, the coordination of the V sites in the mesostructure was found to be exclusively tetrahedral. However, the influence of the vanadium content was not studied.

In this contribution, we will further investigate the effect of the V incorporation on the structural characteristics of the MCM-48 materials and we will characterize the different V species that are formed, distinguishing also the incorporated and surface V species.

Experimental Section

The vanadium-containing MCM-48 molecular sieves were prepared using the 16−12−16 gemini surfactant, as described elsewhere.[4] The molar gel composition of the synthesis mixture is as follows: surfactant/NaOH/H_2O/TEOS = 0.06/0.6/150/1. To synthesize V−MCM-48 materials, vanadyl sulfate pentahy-

* Corresponding author. E-mail: mmathieu@uia.ua.ac.be.
† University of Antwerpen.
‡ K. U. Leuven.

10.1021/jp003126r CCC: $20.00
Published on Web 04/04/2001

drate was dispersed in distilled water and the vanadium source was added dropwise to the entire mixture. The synthesis mixture was stirred for 2 h at room temperature, after which the pH had dropped to approximately 11. Subsequently, the entire solution was put in an autoclave at 100 °C for several days. The resulting solid was obtained by vacuum filtration. A 20 g sample of fresh water was added per gram of product, and the produce was returned to the autoclave at 100 °C for an additional period of time. Finally, the product was calcined in ambient air from room temperature to 550 °C with a heating rate of 2 °C/min. Different V−MCM-48 materials were synthesized with Si/V ratios varying from 20 to 100.

To determine the vanadium loading of the catalysts, the samples were stirred with hot sulfuric acid (2 M) for 30 min. After filtration, H_2O_2 was added to the solution, forming the reddish-brown compound $VO_2(SO_4)_3$. The vanadium concentration was then determined colorimetrically at 450 nm.[21]

X-ray diffraction (XRD) patterns were collected with a Philips PW1840 powder diffractometer (45 kV, 25 mA), using Ni-filtered Cu Kα radiation. Porosity and surface area studies were performed on a Quantachrome Autosorb-1-MP automated gas adsorption system. The calcined samples were degassed for 16 h at 200 °C. Gas adsorption occurred using nitrogen as the absorbate at liquid nitrogen temperatures. Surface areas were calculated using the BET method, and the pore size distribution was calculated using the nonlocal density functional theory (NLDFT).[22] Diffuse reflectance spectra (DRS) in the range of 200−2200 nm were taken on a Varian Cary E UV−vis−NIR spectrophotometer. The spectra were recorded using a halon white reflectance standard. Infrared spectroscopy (FTIR) was done with a Nicolet 5 DBX spectrometer, equipped with a MTEC Photoacoustic cell. Raman spectroscopy (RS) was performed with a Nicolet Nexus FT-Raman spectrometer with a Ge detector. All samples were measured at room temperature in a 180° reflective sampling configuration, with a 1064 nm Nd:YAG excitation laser. Electron spin resonance (ESR) spectra were measured with a Bruker ESP300E spectrometer in X-band (9.5 GHz) with a double rectangular TE_{104} mode cavity at room temperature and at 120 K. The samples for DRS and ESR measurements were thermally treated in a specially designed quartz flow cell with Suprasil windows and a quartz tube for DRS and ESR measurements, respectively.

Results and Discussion

Optimization of the Synthesis Conditions (Synthesis Times). The synthesis time of V−MCM-48 materials is defined as the sum of the cooking time (autoclaving the gel in the mother liquid at 100 °C) and the hydrothermal posttreatment time (autoclaving the precipitate in pure water at 100 °C). Both parameters have a distinct effect on the structure and quality of the final materials. The effect of these synthesis parameters on the structure of the V−MCM-48 is illustrated by the XRD patterns in Figure 1. In this case, the Si/V ratio in the mother gel was kept constant (30), and only the cooking and hydrothermal treatment times were altered. The effect of the cooking time was investigated by keeping the hydrothermal treatment time constant at 3 days. Short cooking times (2−5 days) (Figure 1, diffractograms a and b) result in vanadium-containing MCM-48 materials with less intense XRD reflections, compared with materials with a cooking time of 7 days in basic media (Figure 1c). The cubic unit cell parameter a_0 is calculated by the formula $a_0 = d(h^2 + k^2 + l^2)^{1/2}$, with d the interplanar spacing, as calculated by Bragg's law.

It was shown in an earlier publication[4] that the ordering of the pores could be greatly enhanced by a hydrothermal

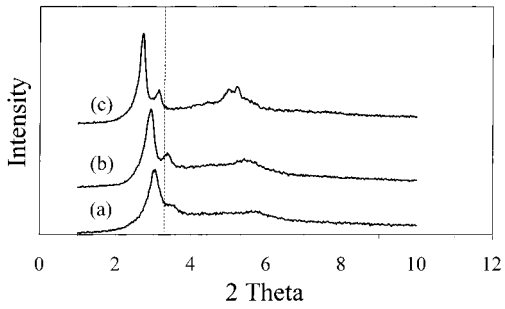

Figure 1. X-ray diffractograms of calcined vanadium MCM-48 prepared by a treatment in base for 2 (a), 5 (b), and 7 days (c) each followed by a hydrothermal treatment of 3 days.

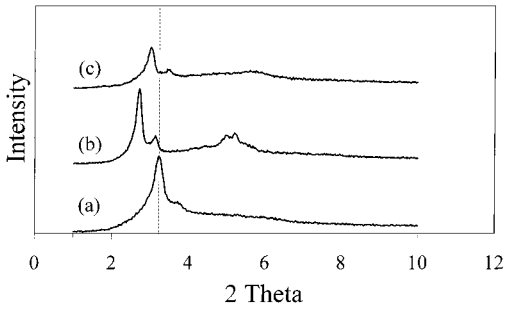

Figure 2. X-ray diffractograms of vanadium MCM-48 materials after calcination. The samples were prepared by a treatment in base for 7 days followed by a hydrothermal treatment of 1 (a), 3 (b), and 5 days (c).

postsynthesis treatment. Resuspending the solid recovered by filtration in distilled water for an additional amount of time lowers the pH of the mother liquor, leading to additional condensation and organization within the walls of the materials.

The XRD patterns in Figure 2 clearly illustrate the effect of this hydrothermal posttreatment step. In this case, the cooking time was kept constant (7 days), followed by a hydrothermal treatment of 1, 3, and 5 days (Figure 2a, 2b, and 2c, respectively). Diffractogram a shows that an autoclaving time of 1 day already results in a mesoporous material with a very high degree of pore ordering, showing the two major reflections in the region $2\theta = 2-4$, which is typical for a MCM-48 molecular sieve. As can be observed, a synthesis time of 7 days in basic media followed by 3 days in water leads to a gradual shift of the (211) XRD peak to lower angles, indicating the enlargement of the unit cell parameter a_0. Also, other reflections in the region $2\theta = 4-7$ become visible, indicating the fine ordering of this vanadium-containing MCM-48 structure. However, a longer hydrothermal treatment decreases the structural ordering, reflecting in a broadening and weakening of the (211) and (220) reflections and the disappearance of the reflections in the region $2\theta = 4-7$. The improvement of the long-range pore ordering upon hydrothermal treatment is attributed to a further condensation and reorganization of the mesoporous framework.[4,6,23]

The vanadium-incorporated MCM-48 structures show not only an excellent ordering (Figures 1 and 2), but also a uniform pore structure, which can be inferred from the sharpness of the step of capillary condensation in the mesopores at $P/P_0 =$ ca. 0.2 (Figure 3A) and the narrow pore size distributions (Figure 3B).

Figure 3A shows the nitrogen adsorption−desorption isotherms for V mesoporous MCM-48 materials obtained after different synthesis times. For all the materials a hysteresis loop was observed extending from relative pressures close to the

TABLE 1: Characteristics of Vanadium-Incorporated and Siliceous MCM-48

gem 16−12−16	days base	days water	S_{BET} (m^2/g)	V_p (mL/g)	D_{DFT} (nm)	a_0 (nm)	t (nm)
A: Physical Characteristics of Calcined V-Incorporated MCM-48 Materials							
V sample 1	1	1	1716	0.85	2.42	6.61	0.88
V sample 2	5	3	1827	1.55	3.21	8.22	1.05
V sample 3	5	5	1800	1.28	2.68	7.09	0.95
V sample 4	7	1	1642	0.85	2.50	6.69	0.91
V sample 5	7	3	1415	1.11	3.03	7.92	1.04
V sample 6	7	5	1516	1.04	2.66	7.14	0.97
B: Comparison between Pure Piliceous and V-Incorporated MCM-48							
blank MCM-48	5	3	1543	1.11	2.85	7.98	0.87
V sample 2	5	3	1827	1.55	3.21	8.22	1.05

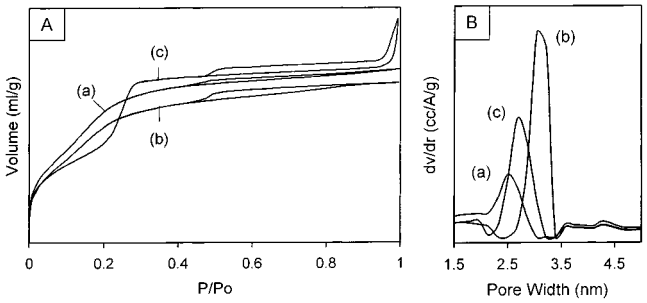

Figure 3. (A) Nitrogen adsorption−desorption isotherms of calcined V−MCM-48 materials after a synthesis time of 1 day in base/1 day in water (a), 2 days in base/1 day in water (b), and 7 days in base/3 days in water (c). (B) Pore size distributions of calcined V−MCM-48 materials prepared by a treatment in base for 7 days followed by a hydrothermal treatment of 1 (a), 3 (b), and 5 days (c).

saturation vapor pressure down to ca. 0.45, at which point they abruptly close. These hysteresis loops developed in the high-pressure range may result from the agglomeration of particles of the mesoporous material. Such an agglomeration of particles was previously reported for MCM-41 materials during aging in the mother liquor.[24] When the hydrothermal treatment is prolonged, the step of capillary condensation in the mesopores becomes sharper and is shifted to higher relative pressures, which indicates a more narrow pore size distribution and a pore size enlargement. This is also clearly illustrated in Figure 3B, where the pore size distributions are shown for the vanadium-containing MCM-48 materials after a synthesis time of 7 days in basic media followed by 1, 3, and 5 days in water (Figure 3B: a, b, and c, respectively). It confirms the narrowing of the pore size distributions and the pore size enlargement as a function of the hydrothermal treatment time.

Table 1A summarizes the physical characteristics of some vanadium-incorporated MCM-48 materials, prepared by the gemini surfactant 16−12−16. It can be noted that high-quality V−MCM-48 materials are obtained, with surface areas exceeding 1000 m^2/g and pore diameters up to 3.2 nm, but with a very narrow distribution. Table 1A illustrates that the hydrothermal treatment has an influence on the unit cell parameter a_0 and that there exists also an optimum value.

A comparison between a pure silica and a vanadium-incorporated MCM-48, prepared under the same synthesis conditions, shows an increase in the unit cell parameter a_0 and in the pore wall thickness t (Table 1B). The pore wall thickness (t) was calculated by the formula $a_0/\xi_0 = t + D_h/2$, with a_0 the unit cell parameter, ξ_0 the reduced area (which is 3.092 for MCM-48), and D_h the hydraulic pore diameter.[22] The enlargement of the unit cell is caused by two simultaneously occurring phenomena: the insertion of the heteroatom with a longer bond distance and the thickening of the pore wall by a transition metal promoted cross-linking of the amorphous silica walls.[10,13,25] The combination of the pore wall thickening and the enlargement of the unit cell therefore is a good first indication for an actual incorporation of the V centers.

TABLE 2: Vanadium Loading and Bulk Si/V Ratio[a]

gem 16−12−16	days base	days water	V concn (wt %)	Si/V (mol/mol)
V sample 1	1	1	1.27	65
V sample 2	5	3	1.67	51
V sample 3	5	5	1.48	56
V sample 4	7	1	2.01	40
V sample 5	7	3	1.34	63
V sample 6	7	5	0.91	91

[a] Si/V ratio in initial mother gel = 14.

Optimization of the Synthesis Conditions (Vanadium Content). The synthesis conditions (cooking time and hydrothermal posttreatment time) do not only affect the structural characteristics of the MCM-48 materials, they also have a pronounced effect on the Si/V ratio of the final materials. This effect is clearly illustrated in Table 2. When the cooking time becomes longer, more vanadium is present in the calcined samples. Also, the duration of the hydrothermal posttreatment plays an important role in the vanadium loading of the obtained V−MCM-48 materials. This table summarizes the vanadium loading, the bulk Si/V ratio, and the synthesis conditions of the calcined V−MCM-48 molecular sieves. All the samples were synthesized, starting from a gel mixture with a Si/V ratio of 14. After a synthesis time of 7 days in basic conditions followed by 1 day in water, the V content is decreased to a Si/V ratio of 40. The vanadium content decreases with increasing hydrothermal treatment time. The decrease in V content can be attributed to a leaching-out effect during the hydrothermal treatment.

The V concentration in the mother gel is obviously another important factor for the final V loading of the calcined V−MCM-48 molecular sieves. Different synthesis times were compared in relation to the V content in the obtained solids and for three different V concentrations in the precursor gel composition. The results are presented in Figure 4A. For all the different synthesis conditions it can be concluded that more vanadium is present in the materials when the Si/V ratio decreases in the gel composition. Also, longer synthesis times result in a relatively higher V content, which might be explained by the thicker pore walls that are created. Comparison between the different synthesis times shows that the V loading is the highest with a synthesis time of 5 days in a base followed by 3 days in water and that a longer hydrothermal treatment results in a decrease of the V content in the materials.

To test the stability of the introduced V centers, the V−MCM-48 materials with a gel composition containing 5.6 wt % vanadium were stirred with liquid water at room temperature for (1 h) to determine the fraction of vanadium centers that is really stable toward leaching. Figure 4B shows that mesoporous materials with a synthesis time of 5 + 3 days retain 30% of the vanadium content present in calcined MCM-48. Extraction with

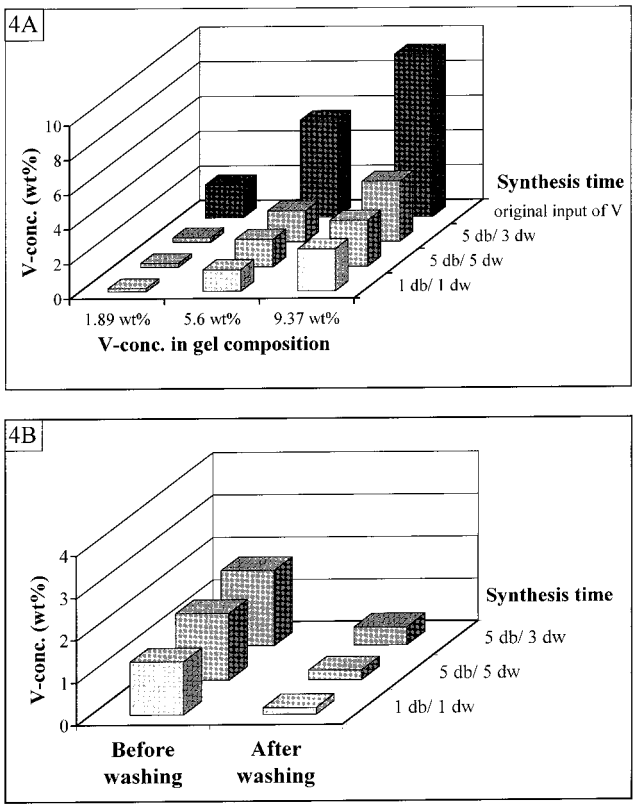

Figure 4. (A) Comparison of the V loading of the obtained V−MCM-48 materials for different synthesis times (2, 8, and 10 days) and for different V concentrations in the precursor gel composition. (B) Comparison of the V content of V−MCM-48 materials before and after stirring with water, for different synthesis times.

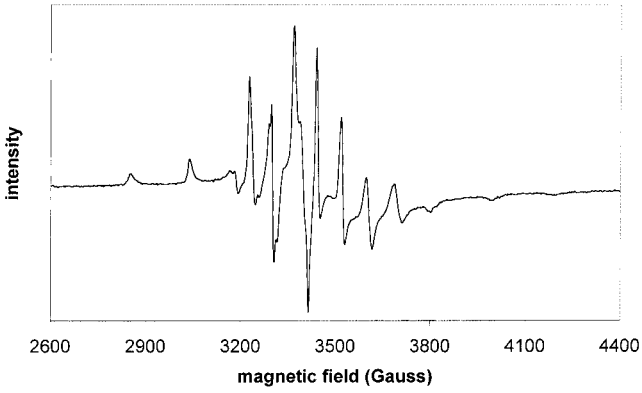

Figure 5. ESR spectrum of as-synthesized V−MCM-48 with a vanadium content of 0.9 wt %.

water of MCM-48 structures prepared by other synthesis times and then 5 days in base followed by 3 days in water results in a loss of more than 90% of the vanadium. For comparison, MCM-48 materials with the VO_x groups grafted at the surface retain no V groups at all after stirring in liquid water for 1 h.[26] Therefore, the V centers that resist this treatment are not surface species. Detailed in situ spectroscopy is employed to further investigate these species.

Spectroscopic Studies. Several spectroscopic techniques were used to gain insight in the coordination environment of vanadium in the MCM-48 material. The ESR spectra of the as-synthesized (uncalcined) V−MCM-48 (Figure 5) exhibit an axially symmetrical signal of tetravalent vanadium, split into a number of hyperfine lines which originate from the d^1 electron interaction with a nuclear spin $I = 7/2$. The well-resolved

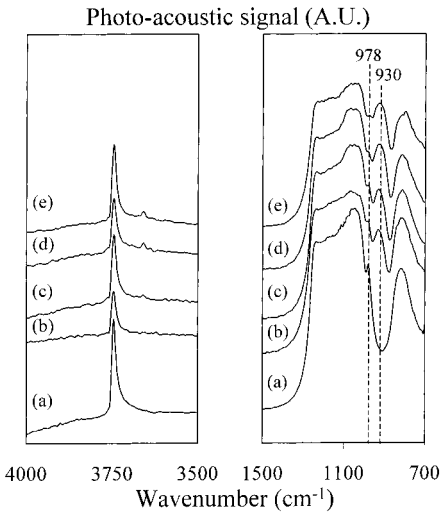

Figure 6. FTIR spectra of a pure silica MCM-48 after calcination (a) and vanadium-incorporated MCM-48 materials with a vanadium content of 0.8 (b), 1.5 (c), 2.6 (d), and 3.5 wt % (e), respectively.

hyperfine structure indicates a very high dispersion of the V^{4+} ions in the sample, as the presence of clusters of framework vanadium ions is usually revealed by a broad line that superposes the hyperfine structure in the ESR spectrum. The signal parameters for the as-synthesized V−MCM-48 material are as follows: $g_{||} = 1.946$, $A_{||} = 184$ G, $g_{\perp} = 1.997$, and $A_{\perp} = 73$ G. It is clear that the obtained g and A values are indicative for the presence of vanadyl ions ($V{=}O^{2+}$) in a distorted pseudo-octahedrally coordinated environment.[27] When the V−MCM-48 material is calcined in a flow of air for increasing temperatures, the total amount of ESR-visible V^{4+} (as obtained by double integration of the V^{4+} ESR signal) gradually decreases with increasing calcination temperature and is zero after calcination at 300 °C (not shown). This indicates that V^{4+} is not very stable against an oxidative treatment in the MCM-48 structure and is readily oxidized to the ESR-silent V^{5+}.

Figure 6 presents the FTIR spectra of pure silica MCM-48 (a) and different calcined vanadium-containing MCM-48 materials with a V loading of 0.8 (b), 1.5 (c), 2.6 (d), and 3.5 wt % (e), respectively. All samples, including the pure silica MCM-48, were prepared by the gemini 16−12−16, after a cooking time of 5 days in the original basic environment followed by 3 days in water. The dominant band at 3745 cm^{-1} is assigned to the O−H stretching of isolated silanols.[28] In the spectra c−e, a small peak appears at 3660 cm^{-1}, assigned to the VO−H stretching vibration.[16,29] A comparison between the spectra indicates that more VOH groups are formed when the V content increases and that a certain amount of vanadium has to be present before the VOH vibration becomes visible. In addition, all spectra of vanadium-incorporated MCM-48 materials reveal the presence of a band at 930 cm^{-1}. This band is attributed to the Si−O−V bonds of VO_x species in the structure of MCM-48 and broadens with increasing V content.[6,18,29,30] The broadening of the band at 930 cm^{-1} is accompanied by the disappearance of the sharp peak at 978 cm^{-1}, which is assigned to the vibration of $Si{-}O^-$ species.[6]

Raman spectra were recorded on V-incorporated MCM-48 samples. Figure 7 shows the Raman spectra of pure V_2O_5 (a), a calcined V−MCM-48 material with a vanadium loading of 2.6 wt % (b), and a blank MCM-48 (c). The Raman bands in Figure 7c at 487 and 609 cm^{-1} (4-fold siloxane rings), 813 and 449 cm^{-1} (siloxane bridges), and 972 cm^{-1} (surface silanol groups), reflecting the features of amorphous-like silica structure,

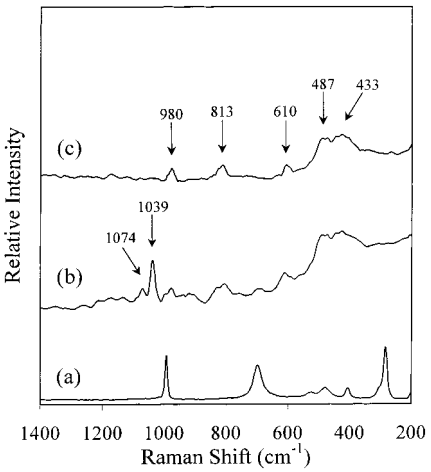

Figure 7. Raman spectra of V_2O_5 (a), V-incorporated MCM-48 with a vanadium loading of 2.6 wt % (b), and pure silica MCM-48 (c).

are due to the pure siliceous MCM-48 framework.[30−32] In the Raman spectrum of V-incorporated MCM-48 the strong band at 1039 cm^{-1} is characteristic for the stretching frequency of terminal V═O groups, tetrahedrally bonded to the silica MCM-48 host.[16,17] Two smaller bands are also observed at ∼1074 and ∼918 cm^{-1}, characteristic for Si−O^- and Si(−O^-)$_2$ functionalities, and can be assigned to perturbed silica framework vibrations, indicative for the formation of V−O−Si entities.[33] The Raman spectra do not show bands at 995, 703, 527, and 404 cm^{-1} characteristic for V_2O_5.[16,17] Therefore, the presence of V_2O_5 clusters can be excluded. In conclusion, the Raman spectra suggest that the V^{5+} species in the calcined MCM-48 material are present as monomeric, tetrahedral structures with the existence of V−O−Si bonds.

Additional structural information on the VO_x species was obtained from in situ UV−vis DRS measurements of the vanadium-incorporated MCM-48 materials. All calcined vanadium-containing MCM-48 samples are white immediately after the calcination. Figure 8 shows the UV−vis DR spectra of vanadium-incorporated MCM-48 materials, which have been deconvoluted to obtain a better understanding of the different VO_x species. Six different bands can be discerned, at 220, 250, 300, 365, 410, and 470 nm, respectively. Up to a vanadium content of 1.3 wt % (Figure 8a), the sample shows exclusive bands in the 200−400 nm region. The band at 220 nm is attributed to the MCM-48 material.[34] Besides the band at 220 nm also two bands with maxima at 250 and 300 nm are observed. These two absorption bands have been assigned to the charge-transfer transitions of V^{5+} species in an isolated tetrahedral environment.[33,35−37] When more than 1.3 wt % vanadium is present in the MCM-48 structure (Figure 8b), a new band at 365 nm appears. The new absorption band at 365 nm is attributed to polymerized, tetrahedral VO_4 species.[33] Furthermore, a shoulder appears in the region 400−500 nm, indicating the presence of square-pyramidal (410 nm) and octahedral (470 nm) V^{5+} species.[33]

After recording the spectrum in ultradry conditions (Figure 8a), the sample with a vanadium content of 1.3 wt % was exposed to water vapor for several hours and a yellow color, which is reversible upon calcination, appears. It is generally accepted that this color change is due to the coordination of two water molecules to the colorless tetrahedral V species, resulting in a distorted octahedral structure.[5,33] It can be inferred from the wetted sample (Figure 8c) that upon water sorption significant absorption occurs in the 300−600 nm region. A comparison with the dry sample (Figure 8a) reveals that the

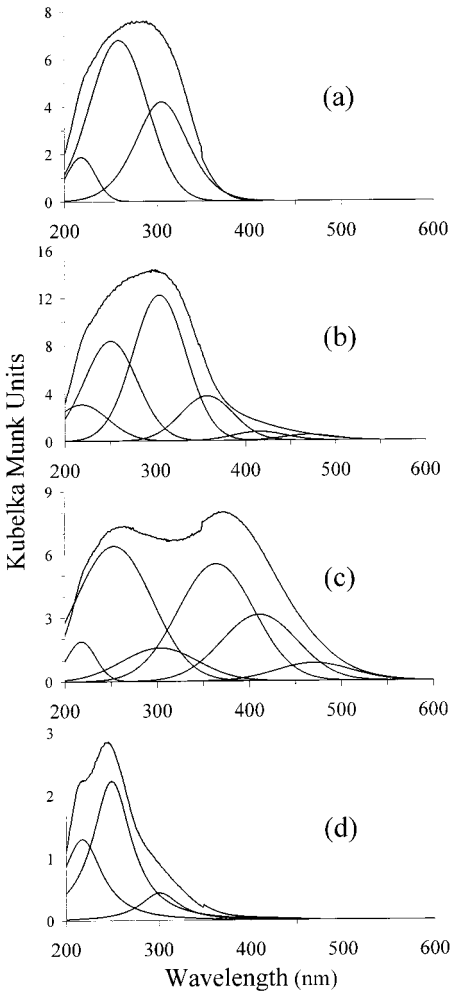

Figure 8. Deconvoluted UV−vis DR spectra of calcined vanadium-incorporated MCM-48 materials: (a) dry V−MCM-48 with 1.3 wt % V; (b) dry V−MCM-48 with 3.5 wt % V; (c) (a) after air exposure for several hours; (d) (a) after stirring with water.

hydration process gives rise to bands at 365, 410, and 470 nm, while the absorption band at 300 nm decreases. The coordination of the V centers during hydration with incorporated and grafted vanadium-containing MCM-48 materials is different. Hydrated grafted vanadium-containing MCM-48 materials[5] reveal the presence of only octahedral VO_x species while hydrated V-incorporated MCM-48 samples show polymerized VO_x species and only a small amount of octahedral species.

To determine which band can be assigned to V^{5+} species incorporated in the framework and vanadium oxides on the external walls of the MCM-48, the sample (Figure 8a) was stirred with water for 1 h. This extraction with water leads to a reduction in the vanadium content with 77%. Figure 8d represents the UV−vis DR spectrum of the calcined sample after stirring with water, and the relative contributions of the deconvoluted peaks at 250 and 300 nm are presented in Figure 9. Although they should be treated semiquantitatively, very interesting trends can be observed. For the dry samples, the relative contribution of the 250 nm band decreases and the contribution of the 300 nm band increases with increasing V loading. Clearly two different species are formed: at low vanadium loading, mainly the 250 nm species is formed; as the V loading increases, their relative contribution becomes smaller in favor of the 300 nm species. Upon hydration of these samples, Figure 9 shows that the 300 nm contribution almost completely disappears, due to the coordination with water, forming polym-

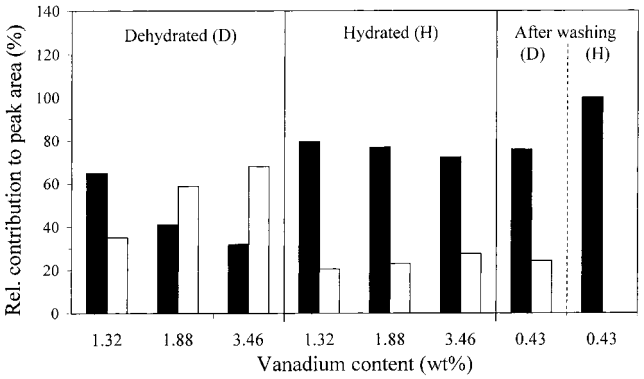

Figure 9. Band deconvolution of 250 (■) and 300 (□) nm contributions in UV−vis DRS in terms of vanadium content.

TABLE 3: Overview of the Formed VO_x Species Present in Dehydrated MCM-48

V content (wt %)	band max. (nm)	molecular structure
<1.5	250, 300	isolated incorporated T_d VO_x (>50%) isolated supported T_d VO_x
>1.5	250, 300	isolated incorporated T_d VO_x isolated supported T_d VO_x (>50%)
>3.5	250, 300, 365, 410, 470	isolated incorporated T_d VO_x (<30%) isolated supported T_d VO_x polymerized T_d VO_x (>10%) square-pyramidal VO_x and octahedral VO_x (<5%)

erized tetrahedral (365 nm), square-pyramidal (410 nm), and octahedral structures (470 nm). The 250 nm contribution however remains virtually constant, and does not decrease significantly after hydration. Finally, the samples that have been stirred with water for 1 h exhibit only a very faint 300 nm feature, indicating that these species have almost completely disappeared. These materials show no difference in the position and intensity of the different charge-transfer bands before and after hydration. The 250 nm contribution does not change upon stirring with liquid water and is not affected by de- or rehydration.

Therefore the 250 nm band can be assigned to an isolated and incorporated tetrahedral V species that does not leach out by stirring in liquid water and that apparently does also not coordinate with water molecules to form octahedral species. The band at 300 nm is then assigned to an isolated, tetrahedral surface structure, easily removed by water treatment and coordinating with water molecules during hydration.

The main results of the spectroscopic studies as a function of the V loading are summarized in Table 3. The presence of each VO_x structure was determined by the band maxima at 250, 300, 365, 410, and 470 nm, corresponding with isolated tetrahedral incorporated, isolated tetrahedral supported, polymerized tetrahedral, square-pyramidal, and octahedral VO_x structures, respectively. It is obvious that there is an optimum for the incorporation of isolated vanadium oxides. At V loadings below 1.5 wt %, more than 60% of the vanadium oxide species are incorporated and more surface species are present when the V loading in the MCM-48 material increases. Furthermore, V^{5+} ions in a polymerized tetrahedral coordination are created when the vanadium content is higher than 3.5 wt %.

Conclusions

Vanadium-containing mesoporous MCM-48 materials were synthesized by in situ incorporation using vanadyl sulfate pentahydrate as the vanadium source. All samples were prepared by using the same surfactant, gemini 16−12−16, eliminating the influence of the chain length and the spacer length of the surfactant on the physical characteristics of the obtained solids. Several structural characterization (XRD and BET) and spectroscopic techniques (ESR, FTIR, RS, and UV−vis DRS) show that a cubic MCM-48 structure incorporated with tetrahedral VO_x species is formed.

Two factors are shown to be critical in controlling the physical characteristics of these catalysts: the synthesis time and the vanadium concentration. The length of the hydrothermal post-treatment is very significant and reaches an optimum after 3 days. The unit cell parameter a_0 and the pore wall thickness t increase as a function of the V loading.

A thorough spectroscopic investigation revealed more information on the vanadium coordination in V−MCM-48. ESR measurements of the as-synthesized and calcined materials show that vanadyl ions, VO^{2+}, are oxidized to V^{5+} in the structure of the MCM-48. Infrared spectroscopy reveals the formation of VOH species and SiOV bonds. The latter is also confirmed by Raman spectroscopy, and a band at 1039 cm^{-1} reveals the presence of terminal V═O groups, tetrahedrally bonded to the MCM-48 host. All vanadium oxides are present in an isolated tetrahedral configuration. When the vanadium content is higher than 3.5 wt %, a fraction of polymerized VO_x species can be observed. The UV−vis DR spectrum of V−MCM-48, after stirring with water for 1 h, shows that still 23% of the isolated incorporated tetrahedral VO_x species are present. The UV−vis DRS charge-transfer band at 250 nm is assigned to incorporated, isolated, tetrahedral $V^{5+}O_4$ species. The species do not leach in liquid water and do not coordinate with water molecules during hydration. The 300 nm band is assigned to isolated, tetrahedral surface species that do leach and do coordinate with water to form distorted octahedral structures. Optimum synthesis conditions yield materials with a maximum of 1 wt % really incorporated V species and 2.5 wt % surface species.

Catalytic studies are now being performed to test the catalytic activity of the incorporated species.

Acknowledgment. M.M. is indebted to the IWT-Flanders-Belgium for a Ph.D. grant. P.V.D.V. and B.M.W. acknowledge the FWO (Fund for Scientific Research, Flanders, Belgium) for positions as senior research assistant. R.R.R. is a junior postdoctoral fellow of the Research Council of K. U. Leuven. The authors thank Mrs. L. Verhoeven and Mrs. F. Quiroz for their aid in the experimental work and for the XRD measurements. This work was sponsored by the FWO (under Research Grant No. G.0446.99) and the Flemish government (under the bilateral agreement BIL 22/96 with Romania).

References and Notes

(1) *Microporous Mesoporous Mater. (Special Issue)* **1999**, 27.
(2) *Mesoporous Molecular Sieves*; Bonneviot, L., Béland, F., Danumah, C., Giasson, S., Kaliaguine, S., Eds; Studies in Surface Science and Catalysis 117; Elsevier Science Publishers: Amsterdam, 1998.
(3) Sayari, A. *Chem. Mater.* **1996**, *8*, 1840.
(4) Van Der Voort, P.; Mathieu, M.; Mees, F.; Vansant, E. F. *J. Phys. Chem. B* **1998**, *102*, 8847.
(5) Morey, M.; Davidson, A.; Eckert, H.; Stucky, G. D. *Chem. Mater.* **1996**, *8* (2), 486.
(6) Morey, M.; Davidson, A.; Stucky, G. D. *J. Porous Mater.* **1998**, *5*, 195.
(7) Van Der Voort, P.; Mathieu, M.; Vansant, E. F.; Rao, S. N. R.; White, M. G. *J. Porous Mater.* **1998**, *5*, 305.
(8) Tuel, A. *Microporous Mesoporous Mater.* **1999**, *27*, 151.
(9) Corma, A. *Chem. Rev.* **1997**, *97*, 2373.
(10) Zhang, W.; Pinnavaia, T. J. *Catal. Lett.* **1996**, *38*, 261.
(11) Wachs, I. E.; Weckhuysen, B. M. *Appl. Catal. A* **1997**, *157*, 67.
(12) Whittington, B. I.; Anderson, J. R. *J. Phys. Chem.* **1993**, *97*, 1032.

(13) Reddy, K. M.; Moudrakaski, I.; Sayari, A. *J. Chem. Soc., Chem. Commun.* **1994**, 1059.
(14) Gontier, S.; Tuel, A. *Microporous Mater*. **1995**, *5*, 161.
(15) Luan, Z.; Xu, J.; He, H.; Klinowski, J.; Kevan, L. *J. Phys. Chem*. **1996**, *100*, 19595.
(16) Schraml-Marth, M.; Wokaun, A.; Pohl, M.; Krauss, H. *J. Chem. Soc., Faraday Trans*. **1991**, *87* (16), 2635.
(17) Scharf, U.; Schraml-Marth, M.; Wokaun, A.; Baiker, A. *J. Chem. Soc., Faraday Trans*. **1991**, *87* (19), 3299.
(18) Weitkamp, J.; Karge, H. G.; Pfeifer, H.; Hölderick, W. *Studies in Surface Science and Catalysis*; Elsevier Science Publishers: Amsterdam, 1994; Vol. 84, p 117.
(19) Kornatowski, J.; Wichterlova, B.; Jirkovsky, J.; Löffler, E.; Pilz, W. *J. Chem. Soc., Faraday Trans.* **1996**, *92* (6), 1067.
(20) Centi, G.; Perathoner, S.; Trifiro, F.; Aboukais, A.; Aïssi, C. F.; Guelton, M. *J. Phys. Chem.* **1992**, *96*, 2617.
(21) Vogel, A. I. *Quantitative Inorganic Analysis*; Longman Group Ltd.: London, 1971; p 790.
(22) Schumacher, K.; Ravikovitch, P. I.; Du Chesne, A.; Neimark, A. V.; Unger, K. K. *Langmuir* **2000**, *16*, 4648.
(23) Huo, Q.; Margolese, D. I.; Stucky, G. D. *Chem. Mater*. **1996**, *8*, 1147.
(24) Grun, M.; Unger, K. K.; Matsumoto, A.; Tsutsumi, K. In *Characterisation of Porous Solids IV*; McEnaney, B., Mays, T. J., Rouquerol, J., Rodriguez-Reinoso, F., Sing, K. S. W., Unger, K. K., Eds.; Royal Society of Chemistry: London, 1997; p 82.
(25) Reddy, K. R.; Ramaswamy, A. V.; Ratnasamy, P. *J. Catal*. **1993**, *134*, 275.
(26) Van Der Voort, P.; Baltes, M.; Vansant, E. F. *J. Phys. Chem*. **1999**, *103*, 10102.
(27) Baltes, M.; Van Der Voort, P.; Weckhuysen, B. M.; Rao, R. R.; Catana, G.; Schoonheydt, R. A.; Vansant, E. F. *Phys. Chem. Chem. Phys*. **2000**, *2*, 2673.
(28) Vansant, E. F.; Van Der Voort, P.; Vrancken, K. C. *Characterization and chemical modification of the silica surface*; Studies in Surface Science and Catalysis 93; Elsevier Science: Amsterdam, 1995.
(29) Van Der Voort, P.; White, M. G.; Mitchell, M. B.; Verberckmoes, A. A.; Vansant, E. F. *Spectrochim. Acta, Part A* **1997**, *53*, 2181.
(30) Chao, K. J.; Wu, C. N.; Chang, H.; Lee, L. J.; Hu, S. *J. Phys. Chem. B* **1997**, *101*, 6341.
(31) Fyfe, C. A.; Gobbi, G. C.; Kennedy, G. J. *J. Phys. Chem*. **1985**, *89*, 277.
(32) Chen, C.; Li, H.; Davis, M. E. *Microporous Mater*. **1993**, *2*, 17.
(33) Gao, X.; Bare, S. R.; Weckhuysen, B. M.; Wachs, I. E. *J. Phys. Chem. B* **1998**, *102*, 10842.
(34) Baltes, M.; Cassiers, K.; Van Der Voort, P.; Weckhuysen, B. M.; Schoonheydt, R. A.; Vansant, E. F. *J. Catal*. **2001**, *197*, 160.
(35) Hazenkamp, M. F.; Van Duijneveldt, F. B.; Blasse, G. *J. Chem. Phys.* **1993**, *169*, 55.
(36) So, H.; Pope, M. T. *Inorg. Chem*. **1972**, *11*, 1441.
(37) Reddy, J. S.; Liu, P.; Sayari, A. *Appl. Catal. A* **1996**, *148*, 7.